DOI 10.5162/irs2017/i2.2

A Low-Cost Spectrometer Based on Stress Induced Birefringence

Florian W. Dietachmayr , Stefan Schallmeiner, Bernhard G. Zagar
JKU Linz, Institute for Measurement Technology, Altenbergerstr. 69, 4040 Linz, Austria
florian.dietachmayr@jku.at

Abstract:
Optical spectrometry is widely used in industrial and scientific contexts. Fourier transform spectrometers have since their invention gradually replaced classical, dispersion based spectrometers. Their advantages are higher luminous efficiency and better wavenumber precision. Conversely, disadvantages are their high cost and stringent mechanical requirements. This paper presents a novel approach on spectroscopy using a stress induced birefringence interferometer instead of the typically used Michelson interferometer set-up. The presented measurement set-up only requires a collimated light source, a medium transparent at the to be analyzed wavelengths with a high photo-elastic constant placed between crossed polarizers, and an area scan camera or a line scan sensor, and has no need for any moving parts. Although the achieved resolution $\Delta\nu = 1265\,\mathrm{cm}^{-1}$ is low the measurements prove that the system in principle works. Finally, improvements regarding the achievable resolution are discussed.

Key words: spectroscopy, stress induced birefringence, convex optimization problem, interferometer

Introduction

Optical spectrometry is widely used in industrial and scientific fields, such as food industry [1], astronomy [2], biology [3], and health care [4].
There are two groups of optical spectrometers: 'classical' spectrometers and Fourier transform (FT) spectrometers.
Classical spectrometers directly record the intensity spectrum of incident light (e. g., by using dispersive components to spatially separate the different wavelengths and measuring the intensity of the wavelength components) [5].
FT spectrometers create two beams with different and variable optical pathlengths of the light to be characterized. Both beams then interfere on a detector. The resulting signal at the detector for monochromatic light with wavelength λ_1 and the intensity of one beam I_{0,λ_1} is given by

$$\begin{aligned} I(x) &= 2I_{0,\lambda_1}\cos^2\left(\pi\frac{x}{\lambda_1}\right) \\ &= I_{0,\lambda_1}\left(1+\cos\left(2\pi\frac{x}{\lambda_1}\right)\right) \end{aligned} \tag{1}$$

where x is the optical path difference [6]. When using polychromatic light with the spectral intensity of one beam $I_{\mathrm{s},0}(\lambda)$, one obtains:

$$\begin{aligned} I(x) &= \int_\lambda I_{\mathrm{s},0}(\lambda)\left(1+\cos\left(2\pi\frac{x}{\lambda}\right)\right)\,\mathrm{d}\lambda \\ &= \overline{I_0}+\tilde{I}_0(x) \end{aligned} \tag{2}$$

where

$$\overline{I_0} = \int_\lambda I_{\mathrm{s},0}(\lambda)\,\mathrm{d}\lambda \tag{3}$$

is a constant offset, independent from the optical path difference x, and

$$\tilde{I}_0(x) = \int_\lambda I_{\mathrm{s},0}(\lambda)\cos\left(2\pi\frac{x}{\lambda}\right)\,\mathrm{d}\lambda \tag{4}$$

is usually referred to as the interferogram. Mathematically, $\tilde{I}_0(x)$ is the cosine transform of $I_{\mathrm{s},0}(\lambda)$. The spectrum can therefore be calculated by computing the inverse cosine transform of $\tilde{I}_0(x)$. Due to the nonideal behavior of FT spectrometers, the interferogram is not necessarily symmetrical, so instead of the cosine transform the FT is used for reconstructing the spectrum [6].
FT spectrometers use interferometers to split the incoming light beam into the two beams. Typically, amplitude division interferometers (e. g., Michelson interferometers) are used, where the optical path difference x is varied by a moving mirror. This setup is prone to mechanical vibrations especially when using the spectrometer at shorter wavelengths [7].
Birefringence interferometers separate the two beams by projecting them onto two perpendicular polarization states and delaying them independently due to a birefringent medium. An analyzer (i. e., a linear polarizer) is used to project them

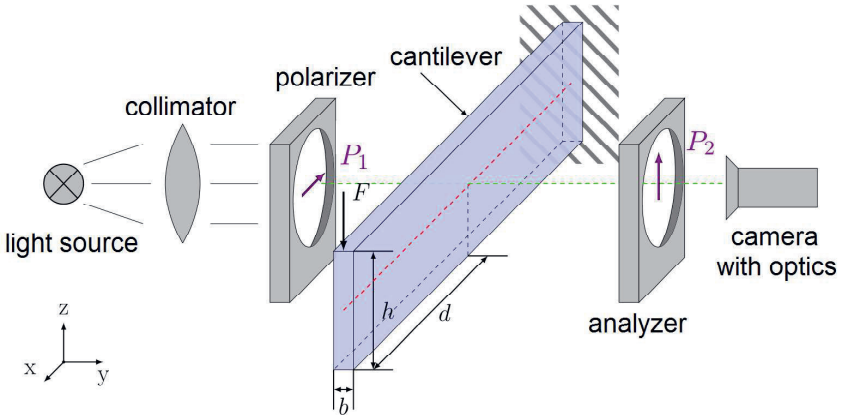

Fig. 1. Schematic of the measurement set-up.

back to a common polarization plane, in order to allow their interference on the detector. An interferogram can similarly be obtained by varying the time-delay and thus the phase-delay due to the birefringent medium (e. g., by changing the thickness of the medium [7] or by using Wollaston prisms [8, 9]). Those spectrometers are better suited for measuring at short wavelengths but still require moving parts.

Many transparent media, when subjected to a mechanical stress, become birefringent, a behavior which is referred to as stress induced birefringence (SIB). The SIB causes an optical path difference x_{SIB} between the two polarization states, which is given by

$$x_{\text{SIB}} = Cb(\sigma_1 - \sigma_2) \tag{5}$$

where C is the photo-elastic constant of the material, σ_1 and σ_2 are the principal stresses in the medium, and b is the thickness of the medium (i. e., the propagation path of the light within the medium orthogonal to the principal stress directions) [10].

By applying a constant force to a transparent material a known stress distribution in the material can be created. Due to the SIB a spatially varying optical path difference x_{SIB} is thus created. Thus, by using an area scan sensor, the interferogram can be measured without the need for any moving parts.

Based on the work in [11], this paper presents a low-cost spectrometer based on SIB. A beam with an applied constant force F is used to generate the known stress distribution.

Measurement Set-up

The measurement set-up consists of a collimated light source (laser JDSU 1135P for calibration and an RGB light emitting diode (LED) YJ503RGB-30B for measurements), a polarizer (polarization plane P_1) and an analyzer (polarization plane P_2) in crossed configuration, a mechanically preloaded cantilever (made from transparent extruded polyethylene terephthalate glycol (PET-G)), and a camera (AVT Prosilica GE1050C) as outlined in Fig. 1. The light is polarized and passes through the cantilever. Due to a constant force F and the resulting stress distribution in the cantilever the SIB causes a spatially varying time-delay between the ordinary and extraordinary wave components along the two principal stress directions. The camera records the emerging fringe pattern.

Figure 2 shows the cantilever from the perspective of the camera (x-z plane). The length of the cantilever is denoted as l, the height as h and the thickness as b (Fig. 1). Due to the resulting stress distribution the interferogram can be measured at vertical lines (see Section 'Mechanical Model'). Thus, a vertical line (through point P) was arbitrarily chosen as evaluation line. The perpendicular distance between the force F and the evaluation line is denoted as d. The directions of the polarization planes of the polarizer and analyzer are denoted as P_1 and P_2, and the angle between the direction of the polarization plane P_1 and the x-axis is denoted as β. The directions of the principal stresses are denoted as σ_1 and σ_2, and the angle between the principal stress direction σ_1 and the x-axis is denoted as θ. Finally, the angle between the direction P_1 and the direction σ_1 is denoted as Φ. Table 1 shows the dimensions of the used cantilever.

Tab. 1: Dimensions of the used cantilever.

name	symbol	value
length of the cantilever	l	109.0 mm
height of the cantilever	h	25.5 mm
width of the cantilever	b	6.0 mm
perpendicular distance between force and evaluation line	d	55.5 mm

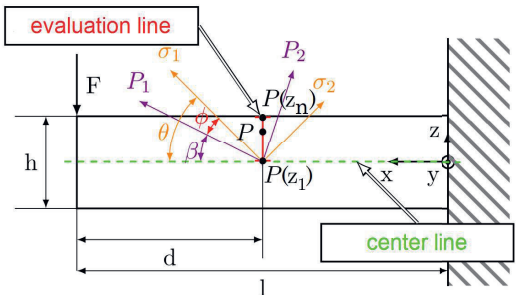

Fig. 2. Cantilever shown from the perspective of the camera (x-z plane).

The intensity of the incident light at the camera's face plate for this configuration is given by

$$I(x_{\mathrm{SIB}}) = \int_{\lambda} 2I_{\mathrm{s},0}(\lambda) \sin^2(2\Phi) \sin^2\left(\pi \frac{x_{\mathrm{SIB}}}{\lambda}\right) \mathrm{d}\lambda \,. \tag{6}$$

By evaluating Eq. (6) on the evaluation line and rewriting it in discrete form, one obtains

$$I(z) = \sum_{\lambda} 2I_0(\lambda) \sin^2(2\Phi(z)) \sin^2\left(\pi \frac{x_{\mathrm{SIB}}(z)}{\lambda}\right) \,. \tag{7}$$

Mechanical Model

The stress distribution in the loaded cantilever must be determined in order to gather useful information from the proposed measurement set-up.
The stress tensor in x-z plane of the loaded cantilever is given by

$$\underline{\sigma} = \begin{bmatrix} \sigma_{xx} & \tau_{xz} \\ \tau_{xz} & 0 \end{bmatrix} \tag{8}$$

with

$$\sigma_{xx} = \frac{M_y}{I_y} z \tag{9}$$

$$\tau_{xz} = \frac{3}{2} \frac{F}{bh} \left(1 - \left(\frac{2z}{h}\right)^2\right) \tag{10}$$

and

$$M_y = Fd \tag{11}$$

$$I_y = \frac{bh^3}{12} \tag{12}$$

where M_y is the bending moment at position d of point P, I_y is the second moment of area, and z is the perpendicular distance between the point P and the center line [12].
To determine the optical path difference x_{SIB} the principal stress components σ_1 and σ_2 have to be calculated. Mathematically, the principal stress components are the eigenvalues of the stress tensor $\underline{\sigma}$ and are given by

$$\sigma_{1,2} = \frac{\sigma_{xx}}{2} \pm \sqrt{\left(\frac{\sigma_{xx}}{2}\right)^2 + \tau_{xz}^2} \tag{13}$$

and the angle of the principal stress direction θ is given by

$$\theta = \frac{1}{2} \arctan\left(\frac{2\tau_{xz}}{\sigma_{xx}}\right) \,. \tag{14}$$

Figures 3 and 4 show the principal stresses and the angle of the pricipal stress direction, respectively, evaluated on the evaluation line. As can be easily seen, the difference $\sigma_1 - \sigma_2$, and therefore the optical path difference, has a minimum above zero. Thus, the measured interferogram will have a missing region around zero. This is problematic when using the Fourier transform to reconstruct the spectrum, as this fact is basically equivalent to an additional convolution of the resulting spectrum with a sinc-function, which further reduces the achievable resolution of the set-up. Therefore, another aproach is used for reconstructing the spectrum: An optimization problem is formulated based on Eq. (7):

$$\min_{\vec{I}_\lambda} \left(|\underline{A}\vec{I}_\lambda - \vec{I}_z|_2^2\right) \tag{15}$$

$$\text{subject to} \quad I_{\lambda_i} \geq 0 \tag{16}$$

where

$$\vec{I}_z = \begin{bmatrix} I(z_1) & I(z_2) & \dots & I(z_n) \end{bmatrix}^T \tag{17}$$

is the vector of the measured intensities along the evaluation line at positions $z_1 \dots z_n$, $\underline{A}$ is the matrix given by the mechanical model with the components

$$A_{i,j} = 2 \sin^2(2\Phi(z_i)) \sin^2\left(\pi \frac{x_{\mathrm{SIB}}(z_i)}{\lambda_j}\right) \tag{18}$$

and

$$\vec{I}_\lambda = \begin{bmatrix} I_{\lambda_1} & I_{\lambda_2} & \dots & I_{\lambda_k} \end{bmatrix} \tag{19}$$

is the spectrum to be calculated. This is a so called convex optimization problem. Every minimum of a convex optimization problem is guaranteed to be a global minimum of the problem [13]. Furthermore, there are a number of different solvers available (e. g., [14]).

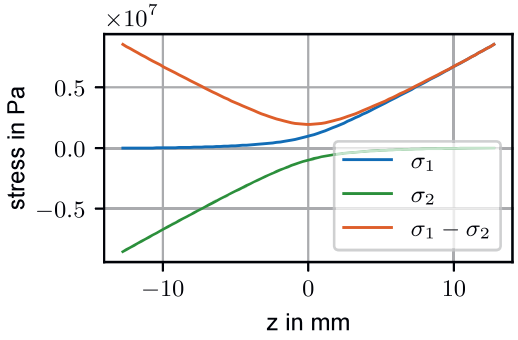

Fig. 3. Principal stresses evaluated on the evaluation line.

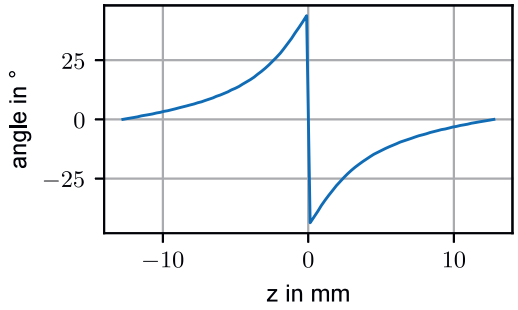

Fig. 4. Angle of the principal stress direction θ evaluated on the evaluation line.

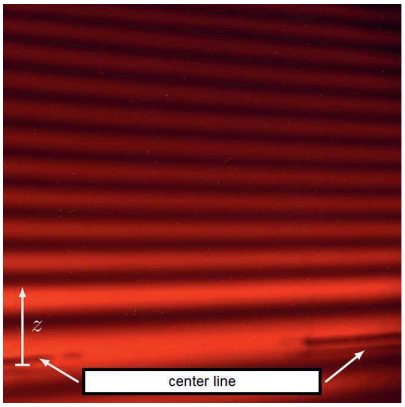

Fig. 5. Measured fringe pattern on the camera using the laser as light source.

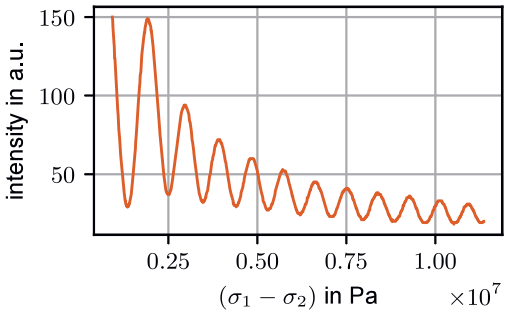

Fig. 6. Measured intensity along the evaluation line using the laser as light source.

Measurement Results

A laser with a wavelength of $\lambda_\mathrm{L} = 632.8\,\mathrm{nm}$ is used for the calibration of the measurement system. Figure 5 shows the measured fringe pattern for an applied force of $F = 100\,\mathrm{N}$. Figure 6 shows the measured intensity along the evaluation line. The optical path difference changes along the evaluation line by appoximately 12.5 periodes, i. e., $\Delta x_\mathrm{SIB} = 12.5\lambda_\mathrm{L} = 7910\,\mathrm{nm}$, and the difference of the principal stress components changes by $\Delta(\sigma_1 - \sigma_2) = 9.1\,\mathrm{MPa}$. The photoelastic constant is therefore given by

$$C = \frac{\Delta x_\mathrm{SIB}}{b\Delta(\sigma_1 - \sigma_2)} = 1.44 \times 10^{-10}\,\mathrm{Pa}^{-1}\,. \quad (20)$$

The wavenumber resolution of the measurement system is given by

$$\Delta\nu = \frac{1}{100\Delta x_\mathrm{SIB}} = 1265\,\mathrm{cm}^{-1}\,. \quad (21)$$

For the evaluation of the measurement system, the spectrum of a collimated RGB-LED is measured by the proposed system and compared to the spectrum measured by a commercial spectrometer. Figure 7 shows the measured intensity evaluated on the evaluation line along with the result of the optimization problem. Figure 8 shows the reconstructed spectrum. For comparison, the spectrum of the RGB-LED was measured with a Fabry-Perot spectrometer (Hamamatsu C10082CAH) and is shown in Fig. 9. The three peaks of the RGB-LED are distinctively visible in the reconstructed spectrum.

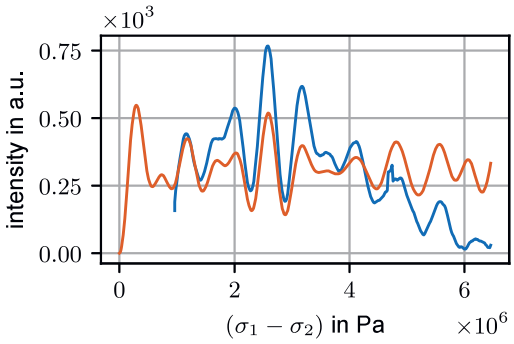

Fig. 7. Measured intensity (blue) and estimated intensity from the optimization problem (red) along the evaluation line using the RGB-LED as light source.

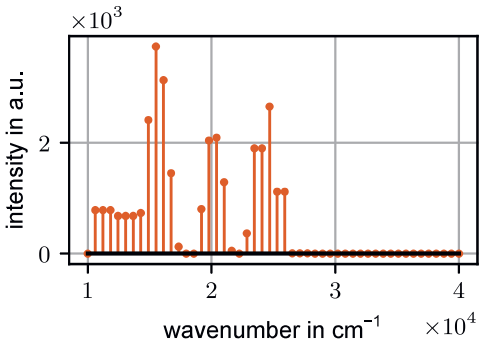

Fig. 8. Estimated spectrum of the RGB-LED from the optimization problem.

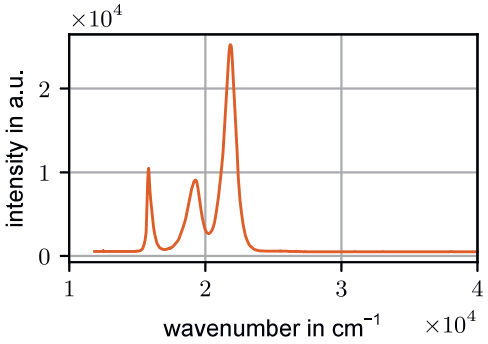

Fig. 9. Measured spectrum of the RGB-LED using a Fabry-Perot spectrometer.

Conclusion

A measurement set-up for a spectrometer based on SIB was presented. Although the achieved resolution is low, the measurement results prove that SIB can be utilized for the construction of a spectrometer. Further investigations will include testing different stress distributions to overcome the problem of the missing region around the zero retardation point in the interferogram and improving the resolution by using different transparent materials. Especially elastomers show a high photo-elastic constant which would increase the achievable resolution [10].

References

[1] W. Wang, J. Paliwal, Near-infrared spectroscopy and imaging in food quality and safety, *Sensing and Instrumentation for Food Quality and Safety*, 1 (2007), no. 4, 193–207, doi:10.1007/s11694-007-9022-0

[2] S. Veilleux, D.-C. Kim, D. B. Sanders, Optical Spectroscopy of the IRAS 1 Jy Sample of Ultraluminous Infrared Galaxies, *The Astrophysical Journal*, 522 (1999), no. 1, 113–138, doi:10.1086/307634

[3] J. Kong, S. Yu, Fourier Transform Infrared Spectroscopic Analysis of Protein Secondary Structures, *Acta Biochimica et Biophysica Sinica*, 39 (2007), no. 8, 549–559, doi:10.1111/j.1745-7270.2007.00320.x

[4] R. K. Sahu, S. Mordechai, Fourier transform infrared spectroscopy in cancer detection, *Future oncology (London, England)*, 1 (2005), no. 5, 635–647, doi:10.2217/14796694.1.5.635

[5] E. Hecht, *Optics*, Pearson, Harlow (2014), ISBN 9781292021577

[6] S. P. Davis, M. C. Abrams, J. W. Brault, *Fourier transform spectrometry*, Academic Press and Elsevier e-books, San Diego (2014), ISBN 9780120425105

[7] F. Preda, A. Oriana, J. Rehault, et al., Linear and Nonlinear Spectroscopy by a Common-Path Birefringent Interferometer, *IEEE Journal of Selected Topics in Quantum Electronics*, 23 (2017), no. 3, 1–9, doi:10.1109/JSTQE.2016.2630840

[8] M. J. Padgett, A. R. Harvey, A static Fourier–transform spectrometer based on Wollaston prisms, *Review of Scientific Instruments*, 66 (1995), no. 4, 2807–2811, doi:10.1063/1.1145559

[9] A. R. Harvey, D. W. Fletcher-Holmes, Birefringent Fourier-transform imaging spectrometer, *Optics Express*, 12 (2004), no. 22, 5368, doi:10.1364/OPEX.12.005368

[10] H. Wolf, *Spannungsoptik: Band 1 · Grundlagen*, Springer Berlin, Berlin (2013), ISBN 9783642808999

[11] S. Schallmeiner, F. W. Dietachmayr, B. G. Zagar, Stress Induced Birefringence Spectroscopy, in *Proceedings of the 2nd International Conference on Sensors and Electronic Instrumentation Advances*, pp. 82–84, International Frequency Sensor Association (IFSA) Publishing, S. L. (2016), ISBN 978-84-608-9963-1

[12] D. Gross, W. Hauger, J. Schröder, et al., *Engineering Mechanics 2: Mechanics of Materials*, Springer-Verlag Berlin Heidelberg, Berlin, Heidelberg (2011), ISBN 9783642128851

[13] S. Boyd, L. Vandenberghe, *Convex optimization*, Cambridge University Press, Cambridge (2015), ISBN 9780521833783

[14] T. F. Coleman, Y. Li, A Reflective Newton Method for Minimizing a Quadratic Function Subject to Bounds on Some of the Variables, *SIAM Journal on Optimization*, 6 (1996), no. 4, 1040–1058, doi:10.1137/S1052623494240456